Non-Metal Redox Kinetics: Oxidation of Bromide Ion by Nitrogen Trichloride

Michael Gazda, Krishan Kumar, and Dale W. Margerum*

Department of Chemistry, Purdue University, West Lafayette, Indiana 47907

Received October 13, 1994[®]

Bromide ion reacts with NCl_3 to generate $NBrCl_2$ with the rate expression $d[NCl_3]/dt = 12[Br^-][NCl_3]$ (M s^{-1} at 25.0 °C, $\mu = 0.50$ M). The $NBrCl_2$ intermediate subsequently reacts with Br^- to give N_2, Br_2, and Cl^- with the rate expression $-d[NBrCl_2]/dt = (0.05 + 5.3[Br^-])[NBrCl_2]$. The overall stoichiometry from pH 3.2 to 6.5 corresponds to $2NCl_3 + 6Br^- \rightarrow N_2 + 3Br_2 + 6Cl^-$. Rate constants for NCl_3 reactions show extreme sensitivity to nucleophilic strength with $SO_3^{2-} > CN^- > I^- \gg Br^-$. Aqueous absorption spectra are determined for NCl_3 with maxima at 336 nm (ϵ 190 M^{-1} cm^{-1}) and 220 nm (ϵ 5320 M^{-1} cm^{-1}) and for $NBrCl_2$ with a maximum at 228 nm (ϵ 4800 M^{-1} cm^{-1}). Spectral bands for NCl_3, $NBrCl_2$, NBr_2Cl, and NBr_3 shift systematically with the number of bromine atoms from 220 to 256 nm. The rate constants for the reactions of $NHCl_2$ with Br_2, HOBr, and Br^- are much larger than that for the reaction of NCl_3 with Br^-.

Introduction

Chlorination of ammoniacal water leads to the formation of chloramine, dichloramine, and trichloramine (nitrogen trichloride).[1,2] These compounds are sources of active chlorine.[3,4] They have been shown to be toxic to fish[5] and to have mutagenic properties.[6] In water treatment, when Cl/N molar dose ratios exceed 1.6, a process known as breakpoint chlorination can occur.[7–9] In this process ammonia is oxidized to N_2 and the active chlorine species are reduced to Cl^-. Dulong[10] prepared trichloramine in 1811 by passing chlorine gas into a solution of an ammonium salt. Pure trichloramine is an oily yellow liquid[11] that is extremely shock and heat sensitive in regard to explosive decomposition, when it is not in aqueous solution.[12,13] Dulong was injured by a violent explosion that occurred during his synthesis of the compound.[10] Trichloramine is volatile (vapor pressure of 150 Torr at room temperature),[14] has limited solubility in water,[14] and possesses an irritating odor. Aqueous trichloramine has spectral absorbance peaks at 336 and 220 nm,[15] but a wide range of molar absorptivities has been reported for this compound (Table 1). Accurate values are difficult to

Table 1. Reported Molar Absorptivity Values for Aqueous NCl_3

λ_{max}, nm	ϵ, M^{-1} cm^{-1}	ref	λ_{max}, nm	ϵ, M^{-1} cm^{-1}	ref
340	260	44, a	336	195 ± 9	34, 18, 19
340	255	15	336	190 ± 3	this work
340	180	b	221	6100	34
337	285	34	220	8100	44
336	272	35	220	5320 ± 90	this work

[a] Huffman, R. P. M.S. Thesis, Purdue University, 1976. [b] Burden, R. P. Ph.D. Dissertation, Harvard University, 1948.

obtain because of the volatility of NCl_3, the variable stoichiometry in its preparation (where HOCl is also present), and the fact that most reducing agents do not have reproducible stoichiometry in their reactions with NCl_3.[16] Several studies[16–19] have shown that sulfite is one reducing agent that reacts quantitatively with NCl_3 to give NH_3, SO_4^{2-}, and Cl^-. This reaction is utilized in the present work to determine reliable values for the molar absorptivity of NCl_3, a constant that is very important in stoichiometric and kinetic studies. Pure NCl_3 cannot be used, and UV absorbance measurement of NCl_3 solutions is the most convenient way to assess its concentration.

The decomposition of NCl_3 in base proceeds by a specific-base/general-acid catalyzed mechanism[20] to yield $NHCl_2$ as an initial product. However, NCl_3 and $NHCl_2$ react rapidly in base to give N_2, OCl^-, and Cl^- as products. The reaction of NCl_3 with $NHCl_2$ was studied separately by Yiin and Margerum[21] and was shown to be general-base catalyzed. This reaction is a key step in the breakpoint chlorination process to form N_2.[21,22] NCl_3 has also been shown to chlorinate organic compounds in aqueous solution.[23]

Bromide ion is frequently found in water systems and is oxidized to HOBr by HOCl.[24] Thus, the reactions of chlor-

* Abstract published in *Advance ACS Abstracts,* June 1, 1995.
(1) Weil, I.; Morris, J. C. *J. Am. Chem. Soc.* **1949,** *71,* 1664–1671.
(2) Palin, A. T. *Waste Water Eng.* **1950,** *54,* 151–159, 189–200, 248–256.
(3) Jolly, W. L. *J. Phys. Chem.* **1956,** *60,* 507–508.
(4) Rosenblatt, D. H. In *Disinfection: Water and Waste Water;* Johnson, J. D., Ed.; Ann Arbor Science: Ann Arbor, MI, 1975; pp 249–276.
(5) Merkins, J. C. *Waste Water Treatment J.* **1958,** *7,* 150.
(6) Shih, K. L.; Lederberg, J. *Science* **1976,** *192,* 1141–1143.
(7) Margerum, D. W.; Gray, E. T., Jr.; Huffman, R. P. In *Organometals and Organometalloids, Occurrence and Fate in the Environment;* Brinckman, F. E., Bellama, J. M., Eds.; ACS Symposium Series 82; American Chemical Society: Washington, DC, 1978; pp 264–277.
(8) Weil, I. W.; Morris, J. C. In *Dynamics of Breakpoint Chorination;* Rubin, A. J., Ed.; Ann Arbor Science: Ann Arbor, MI, 1975; Chapter 13.
(9) Jolley, R. L.; Carpenter, J. H. In *Water Chlorination: Environmental Impact and Health Effects;* Jolley, R. L., Brungs, W. A., Cotruvo, J. A., Cumming, R. B., Mattice, J. S., Jacobs, V. A., Eds.; Ann Arbor Science: Ann Arbor, MI, 1983; Vol. 4, pp 1–47.
(10) Dulong, P. L. Reported by: Thenard, L. J.; Berthollet, C. L. *Ann. Chim. (Paris)* **1813,** *86,* 37–43.
(11) Noyes, W. A.; Haw, A. B. *J. Am. Chem. Soc.* **1920,** *42,* 2167–2173.
(12) Mellor, J. W. *Comprehensive Treatise in Inorganic and Theoretical Chemistry;* Longmans: New York, 1928; p 598.
(13) Kovacic, P.; Lowery, M. K.; Field, K. W. *Chem. Rev.* **1970,** *70,* 639–655.
(14) *The Merck Index,* 9th ed.; Windholz, M., Ed.; Merck: Rahway, NJ, 1976; p 858.
(15) Metcalf, W. S. *J. Chem. Soc.* **1942,** 148–150.

(16) Dowell, C. T.; Bray, W. C. *J. Am. Chem. Soc.* **1917,** *39,* 896–905.
(17) Coleman, G. H.; Buchanan, M. A.; Paxon, W. R. *J. Am. Chem. Soc.* **1933,** *55,* 3669.
(18) Walker, D. M. M.S. Thesis, Purdue University, West Lafayette, IN, 1981.
(19) Hand, V. C. Ph.D. Dissertation, Purdue University, West Lafayette, IN, 1982.
(20) Kumar, K.; Shinness, R. W.; Margerum, D. W. *Inorg. Chem.* **1987,** *26,* 3430–3434.
(21) Yiin, B. S.; Margerum, D. W. *Inorg. Chem.* **1990,** *29,* 2135–2141.
(22) Jafvert, C. T. Ph.D. Dissertation, University of Iowa, 1985.
(23) Bandara, B. M. R.; Hinjosa, O.; Bernofsky, C. *J. Org. Chem.* **1994,** *59,* 1642–1654.
(24) Kumar, K.; Margerum, D. W. *Inorg. Chem.* **1987,** *26,* 2706–2711.

Table 2. Molar Absorptivities for Species of Interest

species	λ_{max}, nm	ϵ, $M^{-1} cm^{-1}$	ref
OBr^-	329	332	a
Br_2	390	175	33
Br_3^-	266	40900	33
HOBr	260	160	35
OCl^-	292	350	35–37, this work
NH_2Cl	243	461	46
$NHCl_2$	294	272	46
NHBrCl	220	2100	45
$NBrCl_2$	228	4800	this work
NBr_2Cl	241	4400	28
NBr_3	256	4600	44

*a* Troy, R. C.; Margerum, D. W. *Inorg. Chem.* **1991**, *30*, 3538–3543.

amines with Br^-, HOBr, and Br_2 are important in water treatment chemistry, particularly in determining the presence of undesirable disinfection byproducts such as residual halamines. These reactions are also important in understanding conditions that might prevent the formation of bromate ion (a known carcinogen[25]).

Reactions of bromide ion with chloramines lead to the possible formation of bromochloramines (NHBrCl, $NBrCl_2$, and $NBrCl_2$)[26–28] and to reactions between chloramines and bromochloramines to form N_2. The reaction of NCl_3 with Br^- is also of interest for comparison with previous studies of NCl_3 reactions with other nucleophiles (iodide ion,[29] sulfite ion,[30] and cyanide ion[31]). These reactions proceed by a Cl^+-transfer mechanism yielding ICl, $ClSO_3^-$, and ClCN, respectively, as the initial products. Bromide ion is a much weaker nucleophile[32] than I^-, SO_3^{2-}, or CN^-; consequently it is expected to have a slower rate of reaction with NCl_3. A Cl^+-transfer mechanism will yield BrCl as an initial product, but recent work[33] shows that BrCl reacts rapidly with Br^- to give Br_2 or with water to give HOBr.

The NCl_3 reaction with excess Br^-, followed by the appearance of Br_2, initially appeared to have simple pseudo-first-order behavior. However, the kinetics are more complex; this work shows that an intermediate species, $NBrCl_2$, forms and decays. Mechanisms are proposed to satisfy the kinetic and stoichiometric data.

Experimental Section

Reagents. Distilled deionized water was used in all experiments. Bromine solutions were prepared by dissolving liquid Br_2 in dilute $HClO_4$ and were standardized spectrophotometrically (Table 2 gives wavelengths and molar absorptivities for species of interest). Bromide-free solutions of $HOBr/OBr^-$ were prepared by mixing equimolar amounts of OCl^- and Br^- at pH 8. The rate constant for the reaction of HOCl with Br^- (eq 1) is 1.55×10^3 M^{-1} s^{-1},[24] and BrCl rapidly

$$HOCl + Br^- \rightarrow BrCl + OH^- \qquad (1)$$
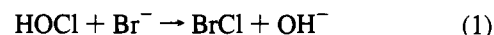
hydrolyzes[33] (eq 2). The HOBr and OBr^- solutions were standardized

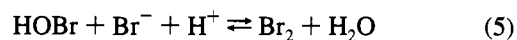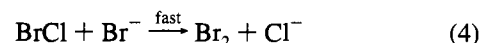$$BrCl + OH^- \xrightarrow{fast} HOBr + Cl^- \qquad (2)$$

spectrophotometrically. Hypochlorite solutions were prepared by dilution of a 10% NaOCl stock solution (Mallinckrodt) and standardized spectrophotometrically. Bromide ion solutions were prepared by dissolving solid NaBr in water and were standardized gravimetrically. Phosphate buffers were prepared by dissolving their sodium salts in water. Acetate buffers were prepared by dilution of glacial acetic acid. Sodium perchlorate solutions were prepared by dissolving recrystallized $NaClO_4$ in water and were standardized gravimetrically. Ammonia solutions were prepared by dilution of concentrated ammonium hydroxide and were standardized by titration with standard HCl.

Preparation of Chloramines. Chloramine (NH_2Cl) solutions were prepared by mixing equimolar amounts of OCl^- and NH_3 at pH 11 and were standardized spectrophotometrically. Dichloramine ($NHCl_2$) solutions were prepared by acidifying NH_2Cl solutions to pH 5 (eq 3).

$$2NH_2Cl + H^+ \rightleftharpoons NHCl_2 + NH_4^+ \qquad (3)$$

The NH_4^+ was removed by cation-exchange chromatography,[34] and any remaining NH_2Cl was separated from $NHCl_2$ via secondary column interactions. Bio-Rad AG50W-X12 100–200 mesh cation-exchange resin was placed in a 2 × 25 cm glass column, protonated with 1 L of 3 M HCl, and equilibrated with 4 L of a solution that was 0.1 M in both $HClO_4$ and $NaClO_4$. The column was rinsed with water until the eluate was at neutral pH. An aliquot of 20 mL of the acidified NH_2Cl solution, originally at 25 mM, was added to the column and eluted at 7.5 mL min^{-1}. The effluent was monitored at 294 nm with a Perkin-Elmer 320 UV–vis spectrophotometer equipped with a low-pressure flow cell. The $NHCl_2$ effluent was standardized spectrophotometrically and was used within 30 min due to its significant decomposition rate.[34]

Solutions of NCl_3 were prepared by T-mixing 3 equiv of HOCl with 1 equiv of NH_3, with both reagents adjusted to pH 4. The reaction mixture was allowed to stand for 18–24 h in the dark with no headspace. The resulting solutions typically contained 5–20% HOCl. The solutions were standardized spectrophotometrically, and the amount of HOCl in the solutions was determined by a kinetic method based on the much faster reaction of Br^- with HOCl[24] than with NCl_3. Data rates on a Hi-Tech stopped-flow spectrophotometer at 400 nm were adjusted to observe bromine when the HOCl reaction with Br^- was essentially complete and the much slower NCl_3 reaction with Br^- was negligible. The absorbance at this point can be used to calculate the $[Br_2]_T$ generated from the $HOCl/Br^-$ reaction (eqs 1 and 2), where $[Br_2]_T$ = [HOBr] + $[Br_2]$ + $[Br_3^-]$ (eqs 4–6).

$$BrCl + Br^- \xrightarrow{fast} Br_2 + Cl^- \qquad (4)$$

$$HOBr + Br^- + H^+ \rightleftharpoons Br_2 + H_2O \qquad (5)$$

$$Br_2 + Br^- \rightleftharpoons Br_3^- \qquad (6)$$

Methods. An Orion Model SA 720 research digital pH meter equipped with a Corning combination electrode was used. The measured pH values were converted to $-\log$ [H^+] at 25.0 °C and μ = 0.50 M on the basis of electrode calibration by titration of standard $HClO_4$ with standard NaOH solution and are reported as p[H^+] values.

A Perkin-Elmer Lambda 9 UV–vis–near-IR spectrophotometer interfaced to a Zenith 386/20 was used to obtain UV–vis spectra and to measure rates of slower reactions.

Faster reactions were measured with either a Durrum or a Hi-Tech stopped-flow spectrophotometer interfaced to a Zenith 151 PC with a Metrabyte DASH-16 A/D interface card. The Hi-Tech instrument was configured in a sequential mixing mode for some reactions.

Ether extraction experiments were carried out by mixing equal volumes of reactants in water followed by extraction of the reaction

(25) (a) Cancer Research Report 1976; Japanese Ministry of Health and Welfare: Tokyo, Aug 1977; pp 744–755. (b) Oikawa, K.; Saito, H.; Sakazume, S.; Fujii, M. *Chemosphere* **1982**, *11*, 953–961. (c) Kurokawa, Y.; Hayashi, Y.; Maekawa, A.; Takahashi, M.; Kokubo, T.; Odashima, S. *JNCI* **1983**, *71*, 965–982. (d) Kurokawa, Y.; Maekawa, A.; Takahashi, M.; Hayashi, Y. *Environ. Health Perspect.* **1990**, *87*, 309–335.

(26) Haag, W. R. *J. Inorg. Nucl. Chem.* **1980**, *42*, 1123–1127.

(27) Gazda, M.; Dejarme, L. E.; Choudhury, T. K.; Cooks, R. G.; Margerum, D. W. *Environ. Sci. Technol.* **1993**, *27*, 557–561.

(28) Gazda, M.; Margerum, D. W. *Inorg. Chem.* **1994**, *33*, 118–123.

(29) Nagy, J. C.; Kumar, K.; Margerum, D. W. *Inorg. Chem.* **1988**, *27*, 2773–2780.

(30) Yiin, B. S.; Walker, D. M.; Margerum, D. W. *Inorg. Chem.* **1987**, *26*, 3435–3441.

(31) Schurter, L. M.; Bachelor, P. P.; Margerum, D. W. *Environ. Sci. Technol.* **1995**, *25*, 1127–1134.

(32) Hine, J. *Physical Organic Chemistry*; McGraw-Hill: New York, 1962; p 161.

(33) Wang, T. X.; Kelley, M. D.; Cooper, J. N.; Beckwith, R. C.; Margerum, D. W. *Inorg. Chem.* **1994**, *33*, 5872–5878.

(34) Hand, V. C.; Margerum, D. W. *Inorg. Chem.* **1983**, *22*, 986–993.

mixture into ether. Nonionic and less polar species were extracted into the ether layer for spectrophotometric analysis.

Molar Absorptivity of NCl₃. Our Hi-Tech stopped-flow instrument is equipped with gastight syringes and is utilized in the method developed for the molar absorptivity determination in which NCl₃ is mixed with excess sulfite. The absorbance of NCl₃ was determined on the Lambda 9 UV—vis spectrophotometer and checked on the Hi-Tech stopped-flow spectrophotometer at 336 nm by pushing this solution against water. The syringe with water was replaced by a glass syringe containing freshly prepared SO_3^{2-} solution. The reaction products, which contained some unreacted SO_3^{2-}, were forced from the receiving syringe into flasks containing 5 mL of standard I_3^- solution. The excess I_3^- was then titrated with standardized $S_2O_3^{2-}$. Six to ten titrations were performed for each experiment. The NCl₃ solution was then removed and replaced with a syringe containing water. After pushing SO_3^{2-} against water, the receiving syringe contents were again forced into flasks containing the I_3^- solution. The excess I_3^- was then titrated with standardized $S_2O_3^{2-}$. This second set of pushes was used to standardize the SO_3^{2-}. Volumes in the receiving syringe were determined by weight and specific gravity values. Hypochlorite ion was used to test the system. This reactant was chosen because it also reacts completely and rapidly with sulfite and because its molar absorptivity has been well characterized.[35-37]
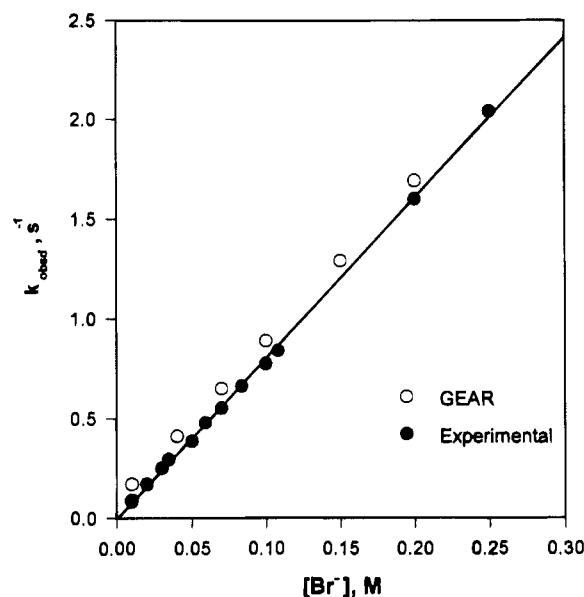
Results and Discussion

Molar Absorptivity of NCl₃. The reaction between NCl₃ and sulfite is given in eq 7. The concentration of NCl₃ in the

$$NCl_3 + 3SO_3^{2-} + 3H_2O \rightarrow$$
$$3SO_4^{2-} + 3Cl^- + 2H^+ + NH_4^+ \quad (7)$$
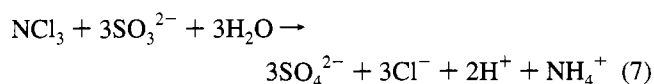
solution was determined by the titration methods described in the Experimental Section, with correction for the [HOCl] present in the NCl₃ solution. A small absorbance contribution from HOCl was taken into account ($\epsilon_{336}(HOCl) \approx 6$ M⁻¹ cm⁻¹). Three sets of NCl₃ solutions were analyzed with seven trials for each set to give a molar absorptivity for NCl₃ at 336 nm equal to 190 ± 3 M⁻¹ cm⁻¹. The molar absorptivity at 220 nm can be calculated from this result as 5320 ± 90 M⁻¹ cm⁻¹. The validity of the procedure was confirmed by using OCl⁻ as a calibrant. The results gave ϵ_{292} for OCl⁻ as 348 ± 11 M⁻¹ cm⁻¹. Since OCl⁻ is not volatile, a separate titration method[38] can also be used; it gave a value of 353 ± 4 M⁻¹ cm⁻¹. These values agree well with the literature value of 350 M⁻¹ cm⁻¹.[35-37] The new molar absorptivity value for NCl₃ at 336 nm is within the experimental uncertainty of our previously determined value of 195 ± 9 M⁻¹ s⁻¹,[18,19,34] but it is measured with greater accuracy and precision. It is more reliable than other previously reported measurements in Table 1, because of the use of a stoichiometric reaction, correction for HOCl content, avoidance of NCl₃ loss due to volatility, and elimination of O₂ which interferes with the triiodide/thiosulfate titration.

NCl₃ + Br⁻ Product Analysis. The reactants were mixed in a T-mixer, and the products were analyzed by UV—vis spectrophotometry. Typical NCl₃ concentrations were 0.2—0.4 mM, while bromide ion concentrations and pH were varied. Aqueous spectra indicated that the bromine-containing product was Br₂/Br₃⁻, and this was confirmed by ether extraction experiments. Table 3 summarizes the conditions and results for the product analysis. The overall stoichiometry of the Br₂ formed relative to initial NCl₃ was 1.4 ± 0.1 from pH 3.2 to

(35) Soulard, M.; Block, F.; Hatterer, A. *J. Chem. Soc., Dalton Trans.* **1981**, 2300—2310.
(36) Gray, E. T., Jr. Ph.D. Dissertation, Purdue University, West Lafayette, IN, 1977.
(37) Johnson, D. W.; Margerum, D. W. *Inorg. Chem.* **1991**, *30*, 4845—4851.
(38) Vogel, A. I. *Vogel's Textbook of Quantitative Inorganic Analysis*, 4th ed.; Longman: New York, 1981; p 382.


Figure 1. Dependence of the pseudo-first-order rate constant (k_{obsd}) on Br⁻ concentration for its reaction with NCl₃ where [Br₂]ₜ formation is observed. The slope of the experimental points (●) is 8.02 ± 0.06 M⁻¹ s⁻¹. The GEAR points (○) are generated from the reaction sequence in eq 15 with typical behavior shown in Figures 5 and 6.

Table 3. Product Analysis for the NCl₃ Reaction with Br⁻

[Br⁻], M	p[H⁺]	[Br₂]ₜ/[NCl₃]	[Br⁻], M	p[H⁺]	[Br₂]ₜ/[NCl₃]
0.010	5.59	1.44	0.100	5.42	1.31
0.020	5.61	1.46	0.100	4.37	1.51
0.050	5.63	1.43	0.100	3.14	1.58
0.106	5.55	1.35	0.100	3.08	1.81
0.106	5.54	1.42	0.100	2.26	2.02
0.106	5.52	1.41	0.100	2.15	2.17
0.159	5.54	1.42	0.100	1.00	2.40
0.266	5.55	1.40	0.100	1.00	2.56
0.100	6.45	1.35	0.100	0.00	2.80
0.100	6.00	1.29			

6.5. This corresponds to the 3/2 ratio for the overall reaction in eq 8. As the pH of the reaction decreases from 3 to 0 (Table

$$2NCl_3 + 6Br^- \rightarrow N_2 + 3Br_2 + 6Cl^- \quad (8)$$
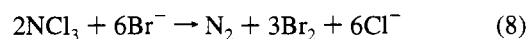
3), the ratio [Br₂]ₜ/[NCl₃] approaches 3 in accord with eq 9,

$$NCl_3 + 6Br^- + 4H^+ \rightarrow NH_4^+ + 3Br_2 + 3Cl^- \quad (9)$$

where NH₄⁺ is the product rather than N₂. Bromine and NH₄⁺ are known to coexist in high [H⁺] and [Br⁻] in equilibria with bromamines.[35] Possible mechanisms for both pH regions are discussed later.

NCl₃ + Br⁻ Kinetics. Kinetics for this reaction were determined by following the formation of products at 400 nm on the Durrum or Hi-Tech stopped-flow spectrophotometer with [NCl₃] typically 0.30—0.70 mM, [Br⁻] = 9.8—250 mM, and p[H⁺] = 3.9—6.1 (acetate or phosphate buffer) or by following the loss of NCl₃ at 336 and 220 nm on the Lambda 9 with [NCl₃] ≃ [Br⁻] ≃ 0.3 mM, p[H⁺] = 5.5—6.9, and 50 mM phosphate buffer. Different results are obtained for the reaction rate constants when the formation of Br₂/Br₃⁻ is monitored at 400 nm (ϵ_{Br_2} = 172 M⁻¹ cm⁻¹, ϵ_{Br_3} = 512 M⁻¹ cm⁻¹) than when the loss of NCl₃ is monitored at 220 or 336 nm. Pseudo-first-order rate constants (k_{obsd}) were obtained for Br₂/Br₃⁻ formation from appropriate fits of the absorbance data at 400 nm vs time in stopped-flow experiments. The dependence of k_{obsd} on bromide ion concentration (Figure 1) gives a second-order rate constant of 8.02 ± 0.06 M⁻¹ s⁻¹. Five of the data points in

Figure 1 were obtained with phosphate buffer at p[H$^+$] 5.5, and the other points were obtained with acetate buffer at p[H$^+$] 5.1. The decay of NCl$_3$ was observed spectrophotometrically under conditions where the bromide ion concentration was sufficiently low to avoid spectral contributions from Br$^-$ or Br$_3^-$. In these experiments the second-order rate constant was determined as 12 ± 2 M^{-1} s^{-1}. Neither the rate of Br$_2$ formation nor the rate of NCl$_3$ loss was affected by pH or buffer concentrations. The discrepancy between these two sets of values for the second-order rate constant is significant. If Br$_2$ formed directly from the NCl$_3$/Br$^-$ reaction, the Br$_2$ formation rate should be 1.5 times faster than the NCl$_3$ decay rate, on the basis of the stoichiometry in eq 8. In fact, the opposite behavior was found. This indicates that Br$_2$ formation must occur via an intermediate species with appreciable concentration.

Further evidence of an intermediate is found when the NCl$_3$ decomposition kinetics is examined at 400 nm under conditions where HOBr is the product. (At this wavelength both NCl$_3$ and HOBr have negligible absorbance.) A small absorbance increase is observed, followed by a decrease at a rate roughly one-half to two-thirds of the rate determined at 336 and 220 nm. On the basis of previous studies[29-31] of NCl$_3$ reactions with nucleophiles, the proposed rate step is nucleophilic attack by Br$^-$ on a Cl atom of NCl$_3$. The resulting Cl$^+$ transfer gives BrCl, and the solvent provides a proton to give NHCl$_2$ (eq 10).

$$H_2O + NCl_3 + Br^- \xrightarrow{k_{10}} OH^- + HNCl_2 + BrCl \quad (10)$$

The BrCl rapidly equilibrates[33] to give HOBr, Br$_2$, and Br$_3^-$ (eqs 2, 4–6). The [Br$_2$]$_T$ generated from eq 10 can react with NHCl$_2$ to give products that subsequently generate more [Br$_2$]$_T$. However, NHCl$_2$ is known to react with NCl$_3$, and NHCl$_2$ could also react with Br$^-$ in a Cl$^+$-transfer step similar to that shown in eq 10. The reaction of NHCl$_2$ with NCl$_3$ at pH 5.5 in phosphate buffer has a rate constant of $\sim$170 M^{-1} s^{-1}.[21] Rate constants for the NHCl$_2$ reactions with Br$^-$ and with [Br$_2$]$_T$ are determined in this work.

NHCl$_2$ + Br$^-$. Immediately after separation on the cation-exchange column, the NHCl$_2$ solution was reacted with bromide ion. The kinetics for the loss of NHCl$_2$ at 294 nm were observed with the Durrum stopped-flow spectrophotometer. The initial dichloramine concentration was typically 0.30 mM, and the [Br$^-$] was 3–15 mM. The p[H$^+$] was maintained at 5.6 ± 0.1 with 50 mM phosphate buffer. The absorbance traces at 294 nm showed a rapid decrease due to loss of NHCl$_2$, followed by a slower increase due to the formation of [Br$_2$]$_T$. Results for the pseudo-first-order rate constants obtained from the absorbance decrease are shown in Figure 2. The slope of this line gives a second-order rate constant at p[H$^+$] 5.6 of 387 ± 27 M^{-1} s^{-1}. The reaction rate increases with a decrease in pH.

The subsequent rate of formation of [Br$_2$]$_T$ has a first-order dependence on [Br$^-$] but does not depend on pH. The second-order rate constant for [Br$_2$]$_T$ formation was 10.8 ± 0.6 M^{-1} s^{-1}. The yield of [Br$_2$]$_T$ relative to the initial [NHCl$_2$] was 0.44 $\pm$ 0.04. The combined yields of this reaction and the reaction in eq 10 give a stoichiometry of $\sim$1.5 for [Br$_2$]$_T$/[NCl$_3$], and the [Br$_2$]$_T$ formation rate is similar to that found in the NCl$_3$/Br$^-$ reaction. However, before any mechanisms are proposed, the NHCl$_2$ reaction with [Br$_2$]$_T$ must be tested.

NHCl$_2$ + Bromide-Free HOBr. The product analysis for the reaction of NHCl$_2$ with bromide-free HOBr was carried out by T-mixing 0.60 mM NHCl$_2$ with 0.60 mM HOBr at pH 6.5 and by examining both the aqueous and the ether extracts by UV–vis spectroscopy. The aqueous reaction product has an absorption maximum at 228 nm, which corresponds to the predicted spectrum for NBrCl$_2$.[26] This compound was formed
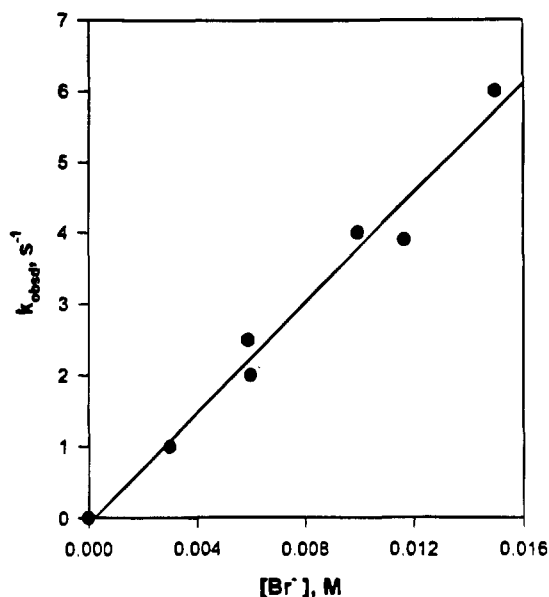

Figure 2. Dependence of the pseudo-first-order rate constant (k_{obsd}) on Br$^-$ concentration for the reaction with NHCl$_2$. The slope of the line is 387 ± 27 M^{-1} s^{-1}.

in the time required (15 s) to place the sample in the spectrophotometer, and its subsequent decay fits second-order kinetics with an initial half-life of $\sim$90 s at p[H$^+$] 6.5. The molar absorptivity of NBrCl$_2$ is estimated to be about 4800 M^{-1} cm^{-1} at 228 nm on the basis of extrapolation of the decay curve to time zero and complete conversion of NHCl$_2$ (eq 11).

$$NHCl_2 + HOBr \xrightarrow{k_{11}} NBrCl_2 + H_2O \quad (11)$$

The kinetics were monitored on the Durrum stopped-flow spectrophotometer by following the formation of NBrCl$_2$ at 240 nm. Initial conditions were [NHCl$_2$] = 0.25 mM, [HOBr] = 0.20 mM, and p[H$^+$] 5.7 with 50 mM phosphate. The formation rate constant (k_{11}) for NBrCl$_2$ was $(9.6 \pm 0.6) \times 10^4$ M^{-1} s^{-1}. The value of this rate constant is a factor of 3 less than the corresponding rate constant for the NH$_2$Cl/HOBr reaction.[28] This is reasonable because NH$_2$Cl is a better Lewis base than NHCl$_2$.

NHCl$_2$ + [Br$_2$]$_T$. Product analysis was carried out by mixing the reactants with a T-mixer and by analyzing the aqueous- and ether-extract UV–vis spectra. Bromide ion was added to the HOBr solutions, which were buffered with 50 mM phosphate at p[H$^+$] 5.6. The analysis showed [Br$_2$]$_T$ as the bromine-containing product. The [Br$_2$]$_T$(final)/[NHCl$_2$](initial) ratio was $\sim$1.5 at p[H$^+$] 5.6 with variable [Br$^-$]. This is expected if the NCl$_3$/Br$^-$ initial reaction products are [Br$_2$]$_T$ and NHCl$_2$.

Kinetics of the reaction were measured on the Durrum stopped-flow spectrophotometer by following Br$_2$/Br$_3^-$ at 400 nm or 266 nm. The bromide ion concentrations varied from 0.1 to 25 mM, and the p[H$^+$] varied from 5.6 to 6.2 with 50 mM phosphate buffer. Concentrations were typically [NHCl$_2$] $\sim$ [Br$_2$]$_T$ $\sim$ 0.3 mM. Figure 3 shows a typical absorbance vs time trace for the reaction. In this figure, the Br$_3^-$ signal is monitored at 266 nm with [Br$^-$] = 5.0 mM. The initial absorbance for this run is $\sim$0.9. The signal decays rapidly and then increases to $\sim$1.5 times the original signal. The decay rate for [Br$_2$]$_T$ increases with increasing [Br$^-$], as does the subsequent reformation of [Br$_2$]$_T$. This is due to increases in the [Br$_2$]/[HOBr] ratios. The data are summarized in Table 4. When the bromide ion concentration is greater than 20 mM, the absorbance decrease can no longer be measured. The resolved rate constant for the reaction of Br$_2$ with NHCl$_2$ is $(5 \pm 2) \times 10^6$ M^{-1} s^{-1}.
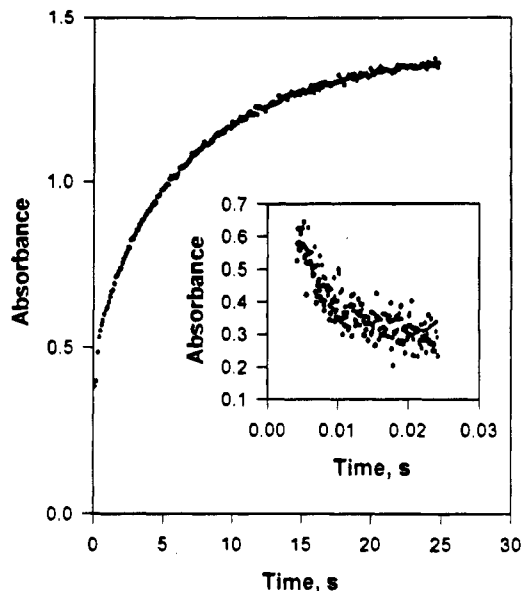
Figure 3. Absorbance trace at 266 nm (1.85 cm cell path) for the reaction of $NHCl_2$ with $[Br_2]_T$. The inset shows the rapid loss of $[Br_2]_T$ in the first 0.02 s. The longer time scale shows the subsequent reformation of ≈ 1.5 $[Br_2]_T$.

Table 4. Data for the Formation and Decomposition of $NBrCl_2$

| $[Br^-]$, M	$p[H^+]$	$10^{-5}k$, M^{-1} s^{-1} $NBrCl_2$ formn[a]	k, M^{-1} s^{-1} $NBrCl_2$ decay	k, s^{-1} Br_2 re-formn
0.00	5.70	0.96 ± 0.06	59 ± 9	
0.0003	5.70	10.9 ± 2.9	153 ± 4	
0.005	5.40	25.9 ± 10.1		0.12[b]
0.005	6.24			0.10[b]
0.005	5.72			0.10[b]
0.010	5.66			0.17[b]
0.020	5.62			0.27[c]
0.025	5.67			0.24[b]
0.050	5.60			0.48[c]
0.050	5.64			0.45[c]
0.050	5.95			0.50[c]
0.050	6.19			0.49[c]

[a] Reaction of $NHCl_2$ with $[Br_2]_T$. [b] Re-formation of Br_2 measured after the reaction of $NHCl_2$ with Br_2. [c] Re-formation of Br_2 measured from the reaction of $NBrCl_2$ with Br^-.

On the basis of the data presented for the reactions of $NHCl_2$ with Br^- and with $[Br_2]_T$, it is evident that in the neutral pH region the reaction of $NHCl_2$ with $[Br_2]_T$ is significantly faster than its reaction with Br^-. Thus, in the NCl_3 reaction with Br^-, the $NHCl_2$ and $[Br_2]_T$ produced react to give $NBrCl_2$ as a product. A subsequent step in the mechanism must be the reaction of $NBrCl_2$ with Br^- to give $[Br_2]_T$ and N_2 as products in the neutral pH region.

$NBrCl_2$ + Br^-. Sequential mixing systems were used to examine this system. The $NBrCl_2$ was generated by pushing one set of syringes that react $NHCl_2$ with bromide-free $HOBr$, both at 0.6 mM. These syringes were then stopped and a second syringe set, containing water in one syringe and Br^- in the other, was started within 2 s. The $NBrCl_2$ was pushed forward by the water and was mixed with the bromide solution (20 and 50 mM Br^-, 50 mM phosphate, pH 5.6). The reaction mixture was then collected and analyzed. The product analysis was performed by aqueous- and ether-extract UV–vis spectrophotometry. The only UV-absorbing product was $[Br_2]_T$. The $[Br_2]_T/[NBrCl_2]$(initial) ratio was ~ 1.5. This is as expected when compared to the NCl_3/Br^- reaction.
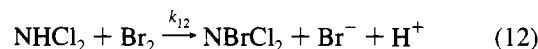
The kinetics of the $[Br_2]_T$ formation were monitored at 410 nm with the Hi-Tech stopped-flow configured in a sequential mixing mode. In these experiments, the $NHCl_2$ was mixed with $HOBr$, a delay time of 3 s was programmed, and then the $NBrCl_2$ was mixed with the bromide ion solutions (10, 25, and
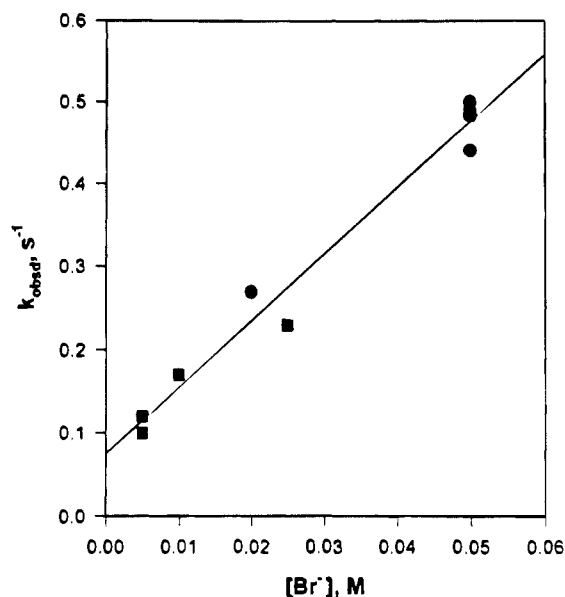
Figure 4. Rate constants as a function of Br^- concentration for the reformation of $[Br_2]_T$ from the reaction of $NHCl_2$ with $[Br_2]_T$ (■) and from the reaction of $NBrCl_2$ with Br^- (●). The slope is 8.0 ± 0.5 M^{-1} s^{-1}, and the intercept is 0.08 ± 0.03 s^{-1}.

50 mM Br^-, 50 mM phosphate, $p[H^+]$ 5.6 to 6.2). The results were first-order traces with no unusual absorbance decrease prior to $[Br_2]_T$ formation. The formation rate increased with increasing $[Br^-]$, and was unaffected by $[H^+]$. This is analogous to the NCl_3/Br^- reaction. The data are summarized in Table 4. Figure 4 is a plot of the combined $[Br_2]_T$ formation data for the $NHCl_2/[Br_2]_T$ reaction and for the $NBrCl_2/Br^-$ reaction. All points fit on the line, regardless of $p[H^+]$. The slope of this line is 8.0 ± 0.5 M^{-1} s^{-1}, with a significant intercept of 0.08 ± 0.03 s^{-1}. The intercept is reasonable, because of the previously discussed decomposition of $NBrCl_2$ in the absence of Br^-. The slope agrees with that found for the $[Br_2]_T$ formation rate when NCl_3 and Br^- were the reactants. Again, these values are different from the rate constant obtained for the decomposition of NCl_3 (12 M^{-1} s^{-1}).
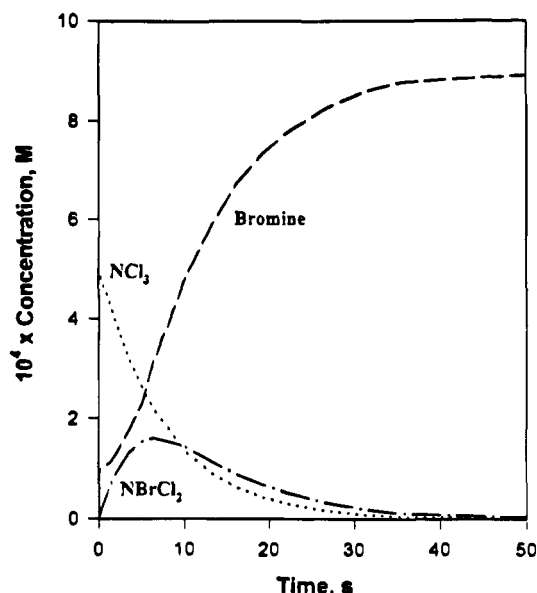
Proposed Mechanisms. After the reaction shown in eq 10, $BrCl$ quickly hydrolyzes (eq 2) or reacts with Br^- to form Br_2 and Br_3^- (eqs 4–6). However, $[Br_2]_T$ species are not observed at this point because of the rapid bromination of $NHCl_2$ (eq 12). It is the subsequent reaction of $NBrCl_2$ with Br^- that

$$NHCl_2 + Br_2 \xrightarrow{k_{12}} NBrCl_2 + Br^- + H^+ \qquad (12)$$

produces Br_2. The proposed steps are shown in eqs 13, 14,

$$H_2O + NBrCl_2 + Br^- \xrightarrow{k_{13}} NHBrCl + BrCl + OH^- \qquad (13)$$

$$3OH^- + NBrCl_2 + NHBrCl \rightarrow$$
$$N_2 + H_2O + 2HOBr + 3Cl^- \qquad (14)$$

and 5 (where Br_2 is formed). Previous work[21,39] has shown that rapid formation of N_2 can occur by the general reaction of NX_3 with NHX_2, where X = Br or Cl. The above reactions lead to an overall ratio of 1.5 $[Br_2]_T$ formed per $[NCl_3]$ in agreement with the experimental observations. In the presence of Br^-, the reaction of $NBrCl_2$ to form Br_2 is first order in both $[NBrCl_2]$ and $[Br^-]$, while in the absence of Br^- the loss of $NBrCl_2$ is second order in $[NBrCl_2]$. Since the $NBrCl_2$ reaction

(39) Inman, G. W., Jr.; LaPoint, T. F.; Johnson, J. D. *Inorg. Chem.* **1976**, *15*, 3037–3042.

Figure 5. GEAR simulation for the reaction of NCl_3 with Br^- using the proposed mechanism for $NBrCl_2$ reaction with Br^-. The initial jump in Br_2 concentration is based on 20% HOCl in the NCl_3 solution.

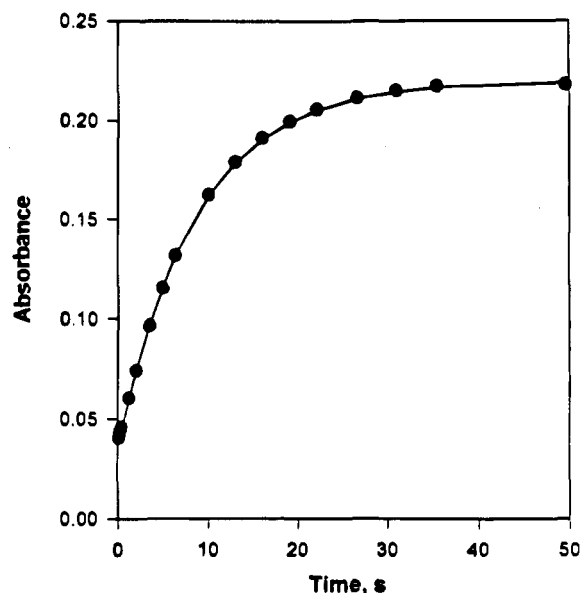**Figure 6.** Simulated absorbance data for $[Br_2]_T$ and $NBrCl_2$ formation at 400 nm for the reaction of NCl_3 with Br^-. The solid line is the apparent first-order fit of the data.

with NHBrCl can be considered as a fast subsequent step, the overall mechanism can be simplified to the sequential reaction shown in eq 15, where $k_{10} = 12$ M^{-1} s^{-1} and $k_{13} = 5.3$ M^{-1}

$$2NCl_3 \xrightarrow[{[Br^-]}]{k_{10}} 2NBrCl_2 \xrightarrow[{[Br^-]}]{k_{13}} 3[Br_2]_T \qquad (15)$$
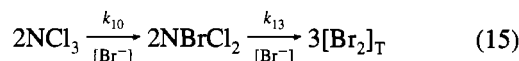
$s^{-1} + 0.05$ s^{-1}. For this mechanism, the $[Br_2]_T$ formation rate constant of 8 M^{-1} s^{-1} is multplied by $^2/_3$ to give the rate constant for loss of $NBrCl_2$ in its reaction with Br^-.

GEAR Simulations. $GEAR^{40,41}$ is a computer program that solves systems of differential equations and can be used to calculate species concentrations as a function of time for multiple reactions. The proposed mechanism discussed above was simulated by the GEAR program and results were compared to the experimental data acquired.

A typical simulation involving eqs 10, 4−6, and 12−14 is shown in Figure 5. Trichloramine undergoes a first-order decay. The bromine concentration increases rapidly initially due to the HOCl (20%) in the NCl_3 solution. After a slight induction period, more Br_2 forms due to the decay of $NBrCl_2$. The $NBrCl_2$ intermediate builds up from the rapid reaction of Br_2 with $NHCl_2$ and then decays as $NBrCl_2$ reacts with Br^-. The $[Br_2]_T$ formation kinetics for the NCl_3 reaction with Br^- were determined by monitoring the absorbance increase. On the basis of the acquired UV−vis spectrum of $NBrCl_2$, there is a significant absorbance contribution from this species at the longer wavelengths, with an estimated molar absorptivity at 400 nm of 150 M^{-1} cm^{-1}. Absorbance data were calculated from the combined contributions of $[Br_2]_T$ and $NBrCl_2$. A typical result is shown in Figure 6. The data fit well to a first-order exponential, as did the experimental data for the NCl_3 reaction with Br^-. The increase in the $NBrCl_2$ concentration appears to offset the induction seen in the $[Br_2]_T$ increase. The rate constants calculated from the GEAR simulation agree well with the experimental results, as shown in Figure 1. The GEAR points are generated by the reaction sequence in eq 15 and give a slope of 7.8 ± 0.2 M^{-1} s^{-1} with a small positive intercept of 0.03 ± 0.025. The experimental results give a second-order rate constant of 8.02 ± 0.06 M^{-1} s^{-1} with zero intercept.

**Alternative Mechanisms. (a) NBr_2Cl Pathway.** In the proposed mechanism, NHBrCl is a reactive intermediate and Br_2 is a product. These species can react with each other to form NBr_2Cl (eq 16).^{26,28} However, this reaction is revers-

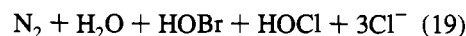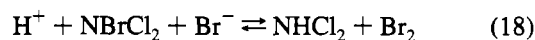$$NHBrCl + Br_2 \rightleftharpoons NBr_2Cl + Br^- + H^+ \qquad (16)$$

ible,^{28,42} and for the conditions used the concentration of NBr_2Cl should be very low. Nevertheless, a possible pathway could involve the reaction of NBr_2Cl with NHBrCl (eq 17). We tested

$$3OH^- + NBr_2Cl + NHBrCl \rightarrow$$
$$N_2 + H_2O + 2HOBr + 2Cl^- + Br^- \qquad (17)$$
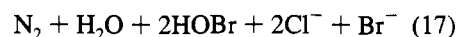
this separately by the use of sequential mixing to react NHBrCl with NBr_2Cl in the presence of 20 and 50 mM Br^- at pH 5.6. The $[Br_2]_T$ formation rate was an order of magnitude slower than experimentally observed in the $NCl_3 + Br^-$ studies. Therefore, the contribution from this pathway can be neglected under our conditions.

(b) $NBrCl_2 + NHCl_2$ Pathway. Another possible path with some of the proposed species is given in eqs 18 and 19.

$$H^+ + NBrCl_2 + Br^- \rightleftharpoons NHCl_2 + Br_2 \qquad (18)$$

$$3OH^- + NBrCl_2 + NHCl_2 \rightarrow$$
$$N_2 + H_2O + HOBr + HOCl + 3Cl^- \qquad (19)$$

Equation 18 is the reverse reaction proposed in eq 12. If it were the rate-limiting step followed by the fast step in eq 19, the reaction would again be first order in $[NBrCl_2]$ and first order in $[Br^-]$ with a second-order rate constant of 5.3 M^{-1} s^{-1}. We also know that the rate constant k_{12} equals 5×10^6 M^{-1} s^{-1}, so we could test these constants in the GEAR program. We found, however, that the resulting simulated data did not agree well with the experimental observations.

(c) $NCl_3 + Br^-$ in Acid. The mechanism for the NCl_3 reaction with Br^- appears to change below pH 3. As the pH decreases, the $[Br_2]_T/[NCl_3]$ ratio approaches 3. This would

(40) Beukelman, T. E.; Chesick, K.; McKinney, R. J.; Weigert, F. J. *GEAR*; E. I. du Pont de Nemours and Co.: Wilmington, DE.

(41) GEAR is a modification of the HAVCHM program; Stabler, R. N.; Chesick, K. *Int. J. Chem. Kinet.* **1978**, *10*, 461−469.

(42) Margerum, D. W.; Gazda, M.; Estes, M. M.; Womback, K. F. To be submitted for publication.
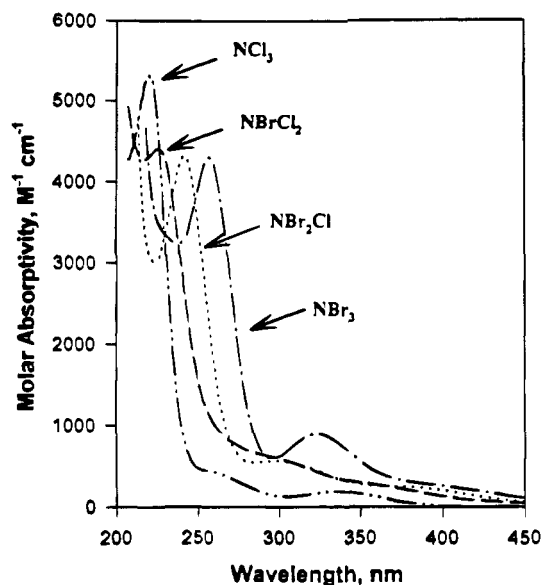
Figure 7. Aqueous UV—vis spectra of the chlorine- and bromine-containing trihalamines.

indicate a complete reduction of the Cl atoms in NCl_3, giving NH_4^+ and Cl^- as products. Bromine and ammonium ion are known to coexist in high acid concentrations in equilibrium with bromamines.[35] We propose that, in high acid concentrations, NHBrCl can react with Br^- as shown in eq 20 to give

$$H^+ + NHBrCl + Br^- \rightarrow NH_2Br + BrCl \qquad (20)$$
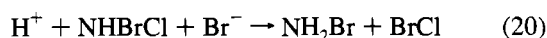
monobromamine and BrCl. Bromine and ammonium ion can then form by the reaction shown in eq 21. The overall reaction is shown in eq 9.

$$NH_2Br + Br^- + 2H^+ \rightleftharpoons NH_4^+ + Br_2 \qquad (21)$$
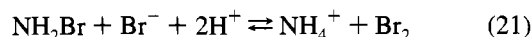
Comparison of the Reactivity of Nucleophiles with NCl_3 and with $NHCl_2$. The rates of reaction of NCl_3 with I^-,[29] SO_3^{2-},[30] CN^-,[31] and Br^- correlate well with the relative nucleophilicities (n)[32] of the anions. The rate constants $(M^{-1} s^{-1}$ at 25 °C) are 4.5×10^9 for SO_3^{2-} $(n = 5.1)$, 1.85×10^9 for CN^- $(n = 5.1)$, 9×10^7 for I^- $(n = 5.04)$, and 12 for Br^- $(n = 3.89)$. Thus, the rate of transfer of Cl^+ from NCl_3 to these anions is extremely sensitive to their nucleophilicity, with a Swain—Scott[43] sensitivity factor, s, of 6.6 for the slope of log k vs n. None of the reactions are acid assisted because NCl_3 is an extremely weak base. This may help to account for the nucleophilic sensitivity.

For SO_3^{2-}, CN^-, and I^- the reactivity of NCl_3 is greater than the reactivity of $NHCl_2$, whereas with Br^- the reactivity of NCl_3 is much less than for $NHCl_2$ at pH 5.6 and $[PO_4]_T = 0.050$ M. The latter reaction appears to be assisted by H^+ and by $H_2PO_4^-$. The reactions of $NHCl_2$ with strong nucleophiles (SO_3^{2-} and CN^-) are not acid assisted while the reactions with weaker nucleophiles (I^- and Br^-) are acid assisted.

Comparison of Trihalamine Aqueous UV Spectra. The UV spectra in aqueous solution are now known for NCl_3, $NBrCl_2$, NBr_2Cl,[28] and NBr_3[44] as shown in Figure 7. The absorbance maxima for the compounds are located at 220, 228, 241, and 256 nm, respectively. This corresponds to a shift to longer wavelengths as the less electronegative bromine atom sequentially replaces chlorine atoms. Figure 8 shows an excellent correlation between the energy of the maximum
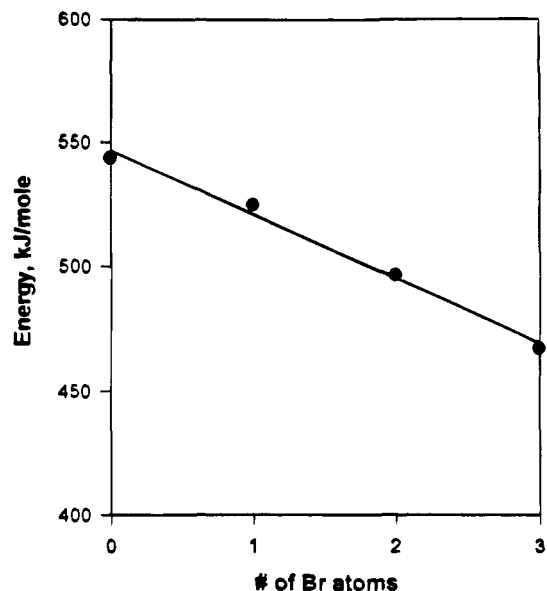
Figure 8. Correlation of the number of bromine atoms in the trihalamine species with the energy of their maximum absorption band. Left to right: NCl_3, $NBrCl_2$, NBr_2Cl, NBr_3.

Table 5. Reactions of Bromide Ion and Bromine-Containing Species in Chlorinated Ammoniacal Water

reaction	rate constant	ref
$H^+ + HOCl + Br^-$	$1.32 \times 10^6 \text{ M}^{-2} \text{ s}^{-1}$	24
$HOCl + Br^-$	$1.55 \times 10^3 \text{ M}^{-1} \text{ s}^{-1}$	24
$NH_3 + HOBr$	$7.5 \times 10^7 \text{ M}^{-1} \text{ s}^{-1}$	a
$NH_2Cl + HOBr$	$2.86 \times 10^5 \text{ M}^{-1} \text{ s}^{-1}$	28
$NH_2Cl + Br_2$	$4.18 \times 10^8 \text{ M}^{-1} \text{ s}^{-1}$	28
$NHCl_2 + HOBr$	$9.6 \times 10^4 \text{ M}^{-1} \text{ s}^{-1}$	this work
$NHCl_2 + Br_2$	$5 \times 10^6 \text{ M}^{-1} \text{ s}^{-1}$	this work
$H^+ + NH_2Cl + Br^-$	$8.9 \times 10^4 \text{ M}^{-2} \text{ s}^{-1}$	b
$NHCl_2 + Br^-$	$357 \text{ M}^{-1} \text{ s}^{-1}$ (pH 5.6)	this work
$NCl_3 + Br^-$	$12 \text{ M}^{-1} \text{ s}^{-1}$	this work
$NBrCl_2 + Br^-$	$5.3 \text{ M}^{-1} \text{ s}^{-1}$	this work
$NBrCl_2 + H_2O$	0.05 s^{-1}	this work
$NHBrCl + HOBr$	$>2 \times 10^3 \text{ M}^{-1} \text{ s}^{-1}$	28

^{a} Wajon, J. E.; Morris, J. C. *Inorg. Chem.* **1982**, *21*, 4258—4263. ^{b} Gazda, M.; Kumar, K.; Margerum, D. W. To be submitted for publication.

absorption band and the number of bromine atoms in the halamine species. The trend is similar with the dihalamine compounds $NHCl_2$, $NHBrCl$,[45] and $NHBr_2$,[44] whose maxima are at 204, 220, and 232 nm, respectively. The large molar absorptivity values of the trihalamines could potentially affect the water analysis for halamines such as NH_2Cl, with a λ_{max} of 243 nm but with a molar absorptivity of only 461 M^{-1} cm^{-1}.[46]

Summary of Water Chlorination Reactions. Table 5 lists some reactions of bromide ion and bromine-containing compounds that may occur in chlorinated ammoniacal water. The precise species distribution and final products formed will vary with Cl/N ratio, $[Br^-]$, and pH. This information should prove useful in modeling water chlorination systems where bromide ion is present. The presence of NH_3 in these systems may inhibit the appearance of bromate ion due to the formation of the various halamine species.

(43) Swain, C. G.; Scott, C. B. *J. Am. Chem. Soc.* **1953**, *75*, 141—147.
(44) Galal-Gorchev, H.; Morris, J. C. *Inorg. Chem.* **1965**, *4*, 899—905.

(45) Trofe, T. W.; Inman, G. W.; Johnson, J. D. *Environ. Sci. Technol.* **1980**, *14*, 544—549.
(46) Kumar, K.; Day, R. A.; Margerum, D. W. *Inorg. Chem.* **1986**, *25*, 4344—4350.